Journal of Cellular Biochemistry 89:720–732 (2003)

Nuclear Distribution of Oct-4 Transcription Factor in Transcriptionally Active and Inactive Mouse Oocytes and its Relation to RNA Polymerase II and Splicing Factors

Vladimir N. Parfenov,[1] Galina N. Pochukalina,[1] Donna S. Davis,[2] Rolland Reinbold,[3] Hans R. Schöler,[3] and Kuruganti G. Murti[2]*

[1]Institute of Cytology, Russian Academy of Sciences, St. Petersburg, Russia 194064
[2]Division of Virology and Department of Infectious Diseases, St. Jude Children's Research Hospital, Memphis, Tennessee 38105
[3]The Center for Animal Transgenesis and Germ Cell Research, University of Pennsylvania, Pennsylvania 19248

Abstract The intranuclear distribution of the transcription factor Oct-4, which is specifically expressed in totipotent mice stem and germ line cells, was studied in mouse oocytes using immunogold labeling/electron microscopy and immunofluorescence/confocal laser scanning microcopy. The localization of Oct-4 was studied in transcriptionally active (uni/bilaminar follicles) and inactive (antral follicles) oocytes. Additionally, the Oct-4 distribution was examined relative to that of the unphosphorylated form of RNA polymerase II (Pol II) and splicing factor (SC 35) in the intranuclear entities such as perichromatin fibrils (PFs), perichromatin granules (PGs), interchromatin granule clusters (IGCs), Cajal bodies (CBs), and nucleolus-like bodies (NLBs). It was shown that: (i) Oct-4 is localized in PFs, IGCs, and in the dense fibrillar component (DFC) of the nucleolus at the transcriptionally active stage of the oocyte nucleus; (ii) Oct-4 present in PFs and IGCs colocalizes with Pol II and SC 35 at the transcriptionally active stage; (iii) Oct-4 accumulates in NLBs, CBs, and PGs at the inert stage of the oocyte. The results confirm the previous suggestion that PFs represent the major nucleoplasmic structural domain involved in active pre-mRNA transcription/processing. The colocalization of Oct-4 with Pol II in both IGCs and PFs in active oocytes (uni/bilaminar follicles) suggests that Oct-4 is intimately associated with the Pol II holoenzyme before and during transcription. The colocalization of Oct-4, Pol II, and SC 35 with coilin-containing structures such as NLBs and CBs at the inert stage (antral follicles) suggests that the latter may represent storage sites for the transcription/splicing machinery during the decline of transcription. J. Cell. Biochem. 89: 720–732, 2003.
© 2003 Wiley-Liss, Inc.

Key words: mouse oocytes; nucleus; immunogold labeling; electron microscopy; Oct-4, RNA polymerase II; splicing factor SC 35

In the last 10 years, considerable progress has been made in understanding the molecular biological aspects of gene expression [for review see Lee and Young, 2000]. Concomitantly, attempts were also made to decipher how this process is spatially organized relative to the distinct compartments/domains that are known to exist in the eukaryotic nucleus [Spector, 1993; Matera, 1999; Gall, 2000; Misteli, 2000]. Biochemical studies have characterized the components of the transcription/splicing machinery and showed that the RNA polymerase II (Pol II) holoenzyme, a multiprotein complex that binds the promoter, consists of the core enzyme RNA polymerase (Pol II), general transcription factors, and the core Srb-mediator complex [Koleske and Young, 1995; Lee and Young, 2000]. Additionally, the carboxy terminal domain (CTD) of Pol II has been implicated in the maintenance of the integrity of the holoenzyme as well as in the coupling of

Grant sponsor: Cancer Center Support (CORE); Grant number: CA-21765; Grant sponsor: American Lebanese Syrian Associated Charities; Grant sponsor: Russian Fund for Basic Research; Grant number: 00-04-49121.

*Correspondence to: Dr. K.G. Murti, Division of Virology and Department of Infectious Diseases, St. Jude Children's Research Hospital, Memphis, TN 38105.
E-mail: gopal.murti@stjude.org

Received 5 February 2003; Accepted 13 March 2003
DOI 10.1002/jcb.10545

© 2003 Wiley-Liss, Inc.

transcription and splicing [Greenblatt, 1997; Mc Craken et al., 1998; Fong and Bentley, 2001]. Immunocytochemical, in situ hybridization and morphological studies, on the other hand, have attempted to identify the intranuclear domains involved in the transcription/splicing [Dundr and Misteli, 2001]. Much, however, remains to be learned concerning the intranuclear distribution of the components of the Pol II holoenzyme and how this multiprotein complex assembles within the nucleus. In this context, there is also a need to understand how transcription factors that are not part of the holoenzyme are recruited to the sites of transcription as well.

In previous studies, we used human oocyte as a model system [Parfenov et al., 1998, 2000] to study the intranuclear distribution of transcription and splicing factors because the system offers stages of development that possess a spectrum of transcriptional activity ranging from active to inert. Using the technique of immunogold labeling/electron microscopy of the oocyte nuclei, we confirmed and extended studies of others by demonstrating that (i) perichromatin fibrils (PFs) represent a nuclear entity in which transcription and splicing are spatially coupled, and (ii) interchromatin granule clusters (IGCs) and nucleolus-like bodies (NLBs) are the storage sites for transcription and splicing machinery.

In the present study, we attempt to localize a key transcription factor, Oct-4, in intranuclear domains of transcriptionally active and inactive mouse oocytes. The reasons for choosing Oct-4 in this study are as follows. First, Oct-4, a transcription factor expressed specifically in the totipotent germ line of mice, maintains the potency of stem and germ cell lines by regulating gene expression [Schöler, 1991; Pesce et al., 1998; Pesce and Schöler, 2000]. Second, Oct-4 represents a transcription factor that is not part of the Pol II holoenzyme. Therefore, it is of interest to analyze how this important transcription factor coordinates its activity in space and time with components of transcription/splicing machinery.

Using immunogold labeling/electron microscopy and immunofluorescence/confocal laser scanning microscopy (CLSM), we determined the sites of distribution of Oct-4 in intranuclear domains of transcriptionally active (uni- and bilaminar follicles) and inactive (antral follicles) oocytes specifically in relation to the intranuclear distribution of components of transcription (Pol II) and splicing (splicing factor SR protein-SC 35) machinery.

METHODS

Oocytes

Ovaries were isolated from 4–5-week inbred BALB/c F1 mice. Ovaries used for immunogold labeling were fixed in 3.7% formaldehyde and 0.1% glutaraldehyde in phosphate-buffered saline (PBS) for 1h. Others were transferred to M2 medium [Quinn et al., 1982] containing 100 μg/ml Dibutyryl cAMP (Sigma, St. Louis, MO) to prevent spontaneous maturation. The cumulus-enclosed oocytes from antral follicles were isolated in Dibutyryl cAMP containing M2 medium by puncturing follicle wall. Oocytes used for immunogold labeling were fixed in 3.7% formaldehyde and 0.1% glutaraldehyde in PBS for 1h and the ones used for immunofluorescence (confocal microscopy) were squashed (see below).

Antibodies

Rabbit anti-Oct-4 polyclonal antibody was obtained, purified, and checked for specificity as described previously [Palmieri et al., 1994]. Monoclonal antibody (Mab), 8WG16, directed against unphosphorylated form of the C-terminal domain (CTD) of RNA Pol II was bought from Research Diagnostics, Inc. (Flanders, NJ). Mab against the SC 35, non-SnRNA splicing factor of pre-mRNA was a gift from Drs. X-D. Fu and T. Maniatis (Harvard University, Cambridge, MA). Rabbit anti-coilin polyclonal antibody against coilin [R-288, Andrade et al., 1993], the marker protein of Cajal bodies (CBs), was kindly supplied by Dr. E.K.L. Chan (The Scripps Research Institute, La Jolla, CA). For immunogold labeling, secondary antibodies conjugated with gold were purchased from Electron Microscopy Sciences, Fort Washington, PA. Secondary antibodies for immunofluorescence (anti-mouse and anti-rabbit FITC- or Texas Red-conjugated IgGs) were bought from Jackson Immunoresearch Laboratories (West Grove, PA).

Immunogold Labeling

Electron microscopy and immunogold labeling were performed as described earlier [Murti et al., 1996; Parfenov et al., 1996]. After

embedding in LR White resin, the ovaries and the oocytes from antral follicles were serially sectioned on a Reichert or Sorvall ultramicrotome. To minimize non-specific binding, the nickel grids with sections were floated on PBS containing 0.5% fish gelatin (15 min). The grids were then floated on primary and secondary antibodies diluted with PBS containing 0.1% fish gelatin for 1.5 h at 37°C. Anti-Oct-4 and 8WG16 antibodies were diluted 1:50 and 1:30, respectively. Anti-coilin was diluted 1:20, and anti-SC 35 was used as undiluted culture supernatant. For double immunogold labeling of Oct-4 and Pol II, the oocyte sections were incubated with anti-Oct-4 followed by goat anti-rabbit IgG conjugated with 15-nm gold particles. After rinsing, the sections were incubated with 8WG16 Mab followed by anti-mouse IgG coupled with 5-nm gold particles. For double immunogold labeling of Oct-4 and SC 35, the sections were sequentially incubated with anti-Oct-4 and goat anti-rabbit IgG conjugated with 15-nm gold particles. After rinsing, the sections were incubated with anti-SC 35 Mab followed by anti-mouse IgG coupled with 5-nm gold particles. For double immunogold labeling of coilin and SC 35, the oocyte sections were sequentially incubated with anti-coilin (rabbit) antibodies and goat anti-rabbit IgG conjugated with 15-nm gold particles. After rinsing, the sections were incubated with anti-SC 35 Mab followed by anti-mouse antibodies coupled with 5-nm gold particles.

The grids were rinsed and stained with 4% aqueous uranyl acetate, and viewed in a JEOL (Japan Electron Optics Ltd., Tokyo, Japan) 1200EXII electron microscope operated at 80 KV. For controls, primary antibodies were omitted from the procedure or irrelevant primary antibodies were used; neither of these controls demonstrated significant labeling.

Immunofluorescence

Before immunofluorescence, oocytes from antral follicles were squashed as described by Bauer and Gall [1997]. The slides with squashed oocytes were dipped in liquid nitrogen and were then placed in 2% paraformaldehyde solution for 30 min. Immunofluorescence was performed as per published procedures [Murti et al., 1996]. The slides with oocytes were incubated with anti-Oct-4, anti-SC 35, 8WG16, or anti-coilin (primary) antibodies, followed by FITC- or Texas-red conjugated secondary antibodies. Anti-Oct-4 and 8WG16 Mab were diluted 1:800 and 1:400, respectively. Anti-SC 35 was diluted 1: 10 and anti-coilin was diluted 1:300. For double immunostaining with anti-Oct-4 and 8WG16 Mabs or anti-SC 35, or anti-coilin and anti-SC 35, the slides with oocytes were sequentially incubated with anti-Oct-4 or anti-coilin (rabbit) antibodies followed by anti-rabbit FITC-conjugated IgGs. After rinsing, the slides were incubated with 8WG16 Mab or anti-SC 35 Mab followed by anti-mouse Texas red-conjugated IgGs. In single labeling experiments with FITC, the slides were also stained with propidium iodide (after incubating with RNase) to stain DNA. Slides double-stained with two primary antibodies at the end of procedure were mounted in PPD mounting medium containing TO-PRO-3 (Molecular Probes, Eugene, OR) to stain DNA.

Confocal Laser Scanning Microscopy

The samples were examined in a Leica TCS NT SP confocal laser scanning microscope equipped with Argon (488 nm), Krypton (568 nm), and Helium–Neon (633 nm) lasers. The three lasers permitted the imaging of FITC (green; emission, 518 nm), Texas red (red; emission, 570 nm), and TO-PRO-3 (far red; emission, 661 nm) fluorochromes, respectively. The samples were examined with 100× plan APO 1.4 NA oil immersion objective. Scanning was performed in X, Y, and Z planes at a laser power of 100% on all lasers at a medium speed setting and at an image size of $1{,}024 \times 1{,}024$ pixels ($1\ \text{pixel} = 0.09\ \mu\text{m}$). The pinhole was set at 1 Airy unit and the photomultiphier tube gain and black levels were set manually to optimize the dynamic range of the image while ensuring that no region was completely suppressed nor completely saturated. Single optical sections (0.5 μm) were obtained through the center of the sample with the averaging function set at 4. When multiple fluorochromes were scanned, the sequential scan function was used to prevent crosstalk between different channels. When collecting Z series, the step size was set at 0.5 μm. The three channel images and an overlay image were recorded using the Leica PowerScan Software and saved as scanner files (tif). The images were re-scaled and gamma corrected with Adobe Photoshop. Three-dimensional reconstruction was done on image series in multipage tif files using the Leica Power Scan software.

RESULTS

The development of mouse ovarian follicles with oocytes has been divided into two phases: (i) growth of the oocyte itself which takes place during the transformation of an unilaminar follicle into plurilaminar follicle, (ii) growth of plurilaminar follicle due to proliferation of the follicular cells, and formation of follicle with the vast antrum. These two phases of follicle development cover 28 days of postnatal life of mouse [Peters, 1969]. It was shown that the process of follicle growth in mouse ovary involves dramatic changes in the transcriptional activity of oocyte nuclei. The total RNA (mRNA and rRNA) synthesis increases in the uni/bilaminar follicle but declines to a minimal level in the antral follicle [Zybina, 1971; Moore et al., 1974; Kaplan et al., 1982]. In the present study, oocyte nuclei at different levels of transcriptional activity from these two stages of follicle development were used to study the dynamics of Oct-4 distribution in relation to Pol II, SC 35, and coilin.

Immunogold Labeling/Electron Microscopy

Uni/bilaminar follicle (active) stage. The general appearance of the oocyte nucleus at this stage is shown in Figure 1. Some of the ultrastructural details described below are not readily visible in this figure but can be seen clearly in Figure 2. The nucleus contains one to two reticulated nucleoli (Fig. 2F) with a well-developed dense fibrillar component (DFC) and fibrillar centers (FC). Several irregular-shaped fibrillogranular bodies are randomly distributed over the nucleus. The fine structure of these bodies (consisting of convoluted fibrils of 6–10 nm in diameter and granules 20–25 nm in diameter, Fig. 2E) corresponds to the IGCs described in mammalian somatic cells [see review Fakan and Puvion, 1980; also see Mintz et al., 1999]. The karyoplasm contains uniformly dispersed chromatin and a number of small patches of condensed chromatin. PFs are often found in association with chromatin, especially at the periphery of the condensed chromatin patches (Fig. 2A) The clumps of chromatin fibrils or PFs are associated with large granules (40–60 nm in diameter) that become more prominent at the antral follicle stage (see below). These granules appear to correspond to perichromatin granules (PGs) described earlier [Daskal, 1981]. The ultrastructural features presented above, such as the reticulated nucleolus with well-defined DFC and dispersed chromatin with well-distinguished PFs, are consistent with the intense transcriptional activity of oocyte nuclei at this stage of the follicle.

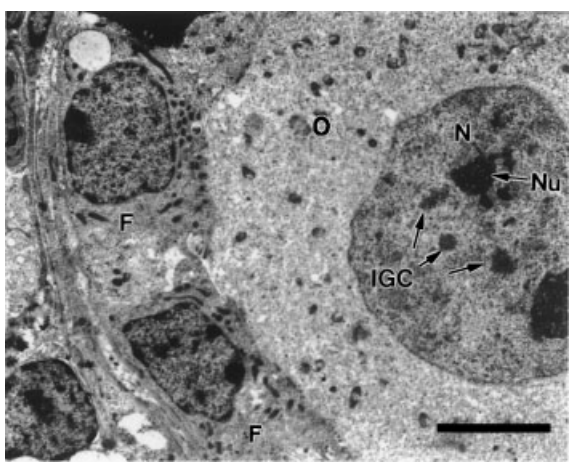

Fig. 1. Part of an uni-laminar mouse follicle with active-stage oocyte. O, oocyte; N, nucleus; Nu, nucleolus; IGC, interchromatin granule clusters; F, follicle cells. Scale bar = 20 μm.

Immunogold labeling of the uni/bilaminar follicles with anti-Oct-4 antibody showed that in oocyte nuclei, this transcription factor is localized on the chromatin and predominantly on PFs (Fig. 2A). To determine the possibility of spatial association between anti-Oct-4 and anti-Pol II, we performed the double immunogold labeling studies with anti-Oct-4 and 8WG16 (anti-Pol II) antibodies using secondary antibodies coupled with different-sized gold particles. The results are shown in Figure 2B. The localization of 8WG16 label in serial sections corresponds to that of anti-Oct-4, both are often found adjacent to each other in fibrillar clumps of chromatin. In the karyoplasm, a similar colocalization between Oct-4 and splicing factor (SC 35) was observed in double labeling experiments (data not shown). The major nuclear components that appear to label with all three antibodies (anti-Oct-4, 8WG16, and anti-SC 35) are the IGCs. The density of labeling of anti-Oct-4 is especially remarkable in large IGCs situated at the periphery of nucleus (Fig. 2C). Double labeling with anti-Oct-4 (small gold particles) and anti-SC 35 (large gold particles) revealed an association of both labels on IGCS (Fig. 2D). Double labeling also revealed an accumulation of the unphosphorylated form of Pol II and Oct-4 in IGCs (Fig. 2E). Detailed analysis of Oct-4, Pol II, and SC 35 distribution inside IGCs showed that they were usually

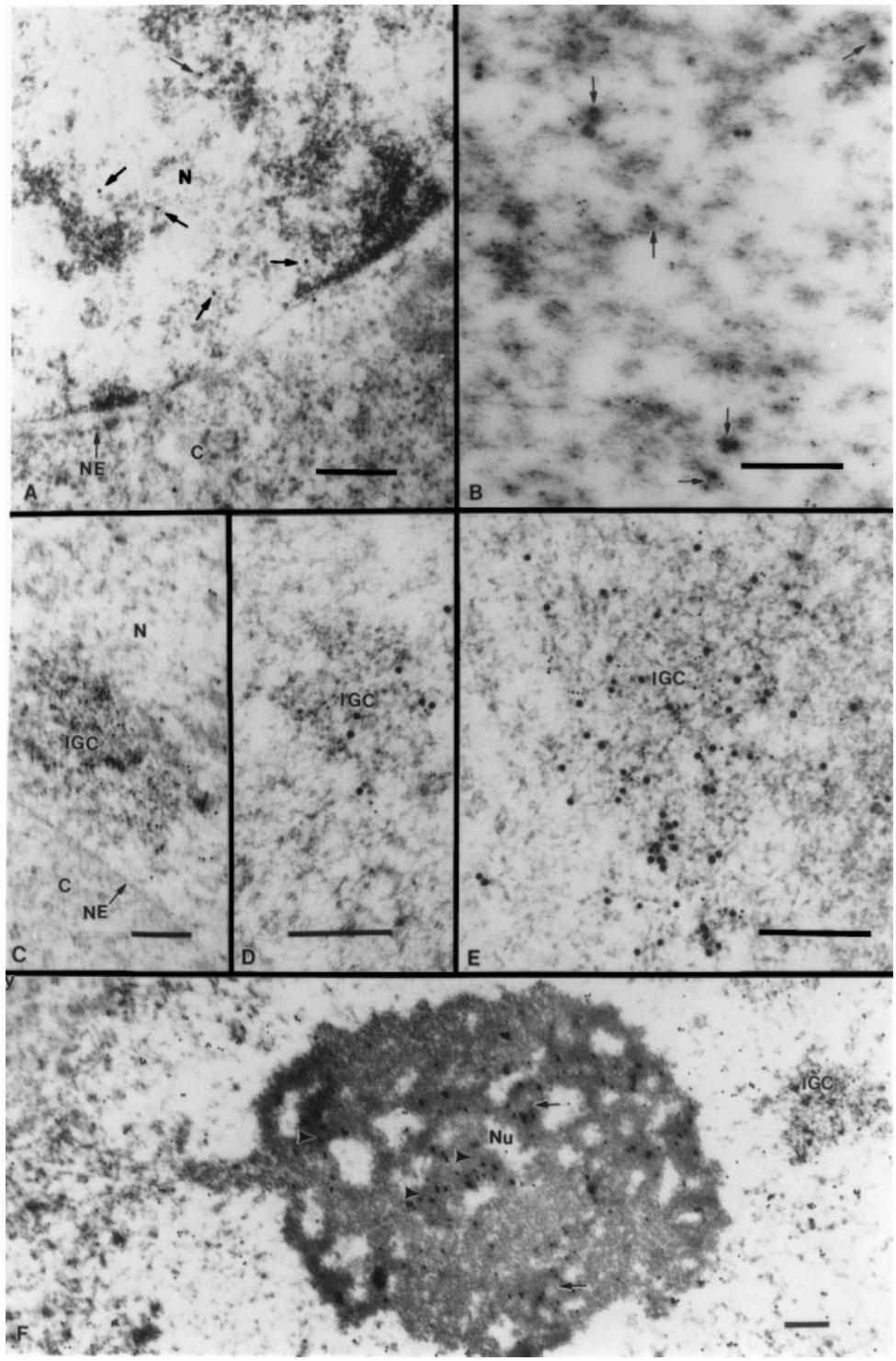

Fig. 2. Immunogold labeling of the nucleus of active-stage oocyte with anti-Oct-4 antibody, anti-Pol II antibody (8WG16), and anti-SC 35. **A**: Labeling of the karyoplasm with anti-Oct-4. Note the localization of label on chromatin connecting the perichromatin fibrils (PFs) and chromatin associated with them (arrows). N, nucleus; C, ooplasm; NE, nuclear envelope. Scale bar in this figure and subsequent figures is 0.25 μm unless otherwise noted. **B**: Double-immunogold labeling of karyoplasm with rabbit anti-Oct-4 antibody (small gold particles) and monoclonal anti-PoII (8WG16) antibody (large gold particles). Note the colocalization of two labels in the fibrillar material (arrows). **C**: Labeling of an IGC located at the nuclear perphery with anti-Oct-4 antibody. N, nucleus; C, ooplasm; NE, nuclear envelope. **D**: Double-immunogold labeling of IGC with anti-Oct-4 antibody (small gold particles) and anti-SC 35 (large gold particles). **E**: Double-immunogold labeling of IGC with anti-Oct-4 antibody (small gold particles) and anti-Pol II(8WG16) antibody (large gold particles). **F**: Part of nucleus with nucleolus (Nu) and IGC after immunogold labeling with anti-Oct-4 antibody. Note the labeled dense fibrillar component—DFC (arrowheads) and fibrillar centers—FCs (arrows) in nucleolus.

associated with the granular component of IGCs. An unexpected result in this study is the association of Oct-4 with the nucleolus (Fig. 2F). The label was consistently seen associated with the DFC of nucleolus; neither the granules nor the FC showed label. Immunogold labeling performed with anti-coilin antibodies on serial sections of oocyte nuclei of uni/bilaminar follicle stage did not reveal any preferential accumulation of coilin in any of the nuclear entities. Anti-coilin showed a diffuse pattern of distribution in the karyoplasm of oocytes (data not shown).

Antral follicle (inert) stage. The general nuclear morphology of oocytes from mouse antral follicles is shown in Figure 3. The nucleus contains a large non-vacuolated, dense nucleolus-like body (NLB) approximately 9–12 μm in diameter, and several less dense spherical nuclear bodies reaching 4–8 μm in diameter. NLB, which is composed of homogenous filamentous material, is a product of nucleolus transformation, which occurs during the mammalian oocyte growth and reflects the reduction of rRNA synthesis [Antoine et al., 1988; Szöllösi et al., 1991; Kopecny et al., 1996; Parfenov et al., 1998, 2000; Zatsepina et al., 2000]. Spherical bodies consisting of fibrils (6–10 nm in diameter) and granules (20–25 nm in diameter) occur in different parts of the nucleus. Few small irregular-shaped nuclear bodies with the same fine structure are dispersed throughout the nucleus. Patches of chromatin of varied levels of condensation are found associated with intranuclear bodies. Chromatin fibrils make close contacts with large granules (40–60 nm in diameter) occurring either singly or in clusters. DNA labeling studies confirmed that the fibrils indeed contain DNA (data not shown). The large granules correspond to the PGs from active stage oocytes of uni/bilaminar follicles (see above). The size, number, the intranuclear location of NLBs, spherical nuclear bodies, and level of chromatin condensation around NLB show some variability in oocytes from different antral follicles. These differences may reflect different steps of oocyte development up to acquisition of competence for nuclear maturation in the end of preovulatory period. At this period, large spherical fibro-granular bodies shrink and disappear and the chromatin condenses around NLB. Our observations on the dynamics of nuclear morphology in oocytes from antral follicles are consistent with earlier observations [Chouinard, 1975; Debey et al., 1993].

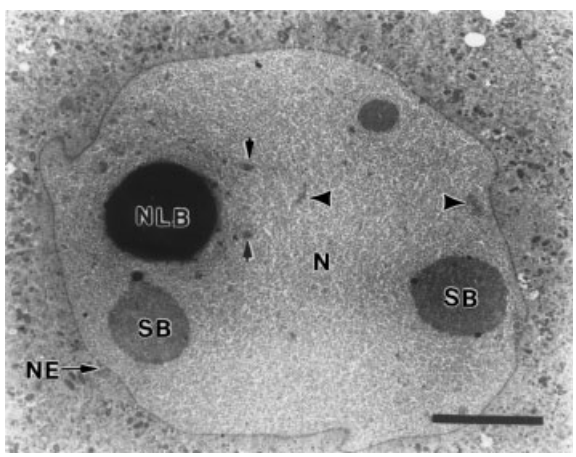

Fig. 3. General nuclear morphology of the inert-stage oocyte from mouse antral follicle. N, nucleus; NE, nuclear envelope; NLB, nucleolus-like body; Chromatin (large arrowheads); SB, spherical nuclear bodies; Irregular-shaped nuclear bodies (small arrowheads). Scale bar is 20 μm.

Immunogold labeling was performed with four antibodies, i.e., anti-Oct-4, anti-SC 35, 8WG16 Mab, and anti-coilin. Oct-4 displayed a noticeable accumulation in antral follicle NLBs (Fig. 4A) Inside NLB, Oct-4 shows a relatively uniform pattern of distribution. Double-labeling experiments with anti-Oct-4 and anti-Pol II (8WG16) antibodies revealed that at this stage labels of both Oct-4 and Pol II occur in NLBs in close association, interspersed with each other in some cases (Fig. 4B). The pattern of 8WG16 labeling of NLBs differs from that of Oct-4. In contrast to uniform anti-Oct-4 labeling, it is observed in the form of irregular patches (Fig. 4B). A remarkable feature of the anti-Oct-4 labeling is its clear association with clusters of large (40–60 nm) granules, which correspond to PGs. Oct-4 label is present in PGs joined by chromatin to the NLB as well as the PGs located in different zones of karyoplasm (Fig. 4C). The next entities intensively labeled with anti-Oct-4 are spherical granular nuclear bodies. As observed in serial sections, most of the labeling is adjacent to 20–25 nm granules. This zone also includes splicing factors (SC 35) as revealed in double labeling experiments (Fig. 4D).

In the karyoplasm, the sparse anti-Oct-4 label is predominantly associated with diffuse fibrillar material. A similar pattern of karyoplasmic labeling was seen with anti-SC 35 as well. Double-labeling studies on serial sections show, that in most cases, the anti-Oct-4 labeling

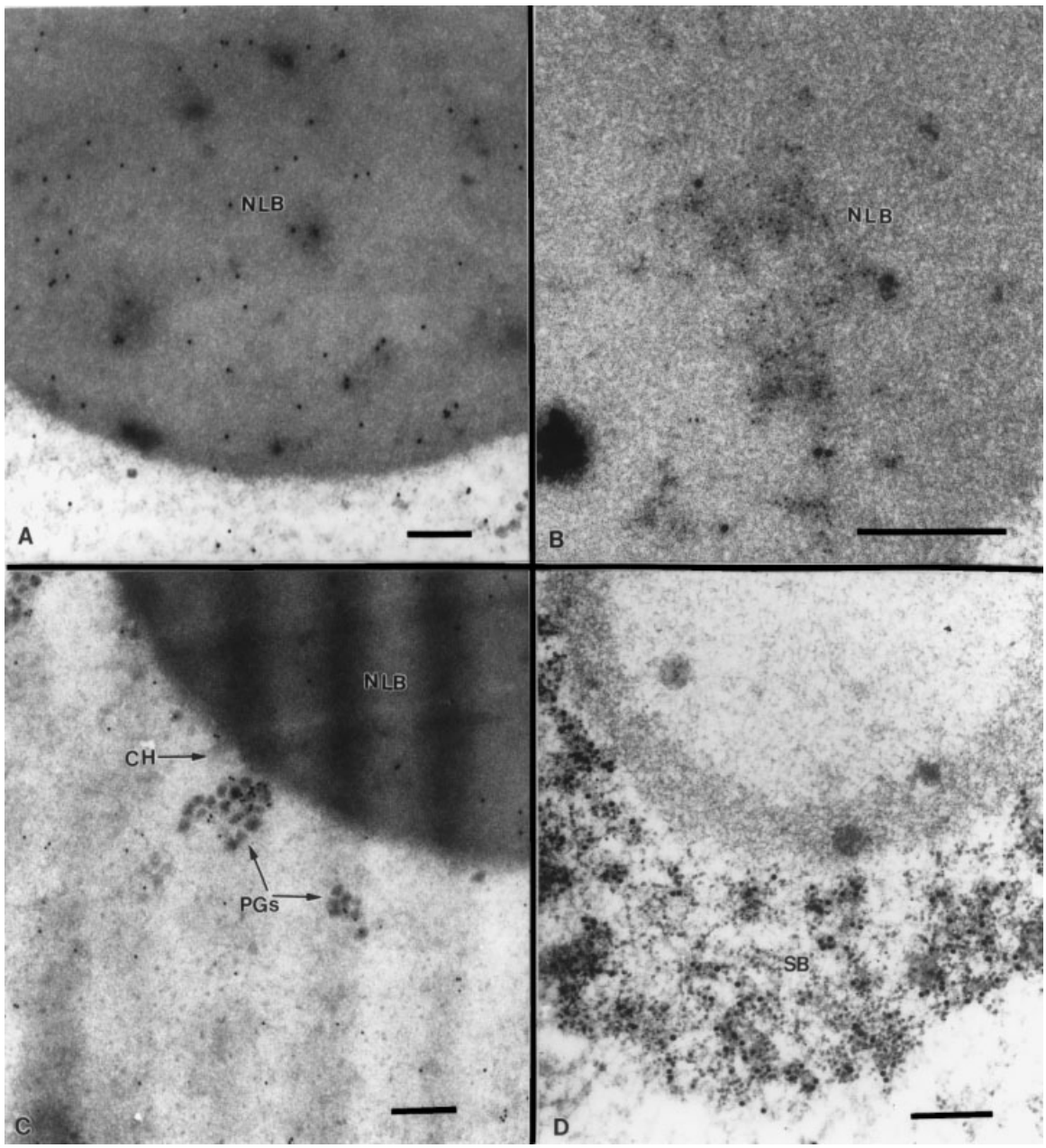

Fig. 4. Immunogold labeling of the nucleus of inert-stage mouse oocyte from antral follicle with anti-Oct-4, anti-Pol II (8WG16), and anti-SC 35 antibodies. **A**: Labeling of NLB with anti-Oct-4. **B**: Double-immunogold labeling of NLB with anti-Oct-4 antibody (large gold particles) and anti-Pol II (8WG16) (small gold particles). **C**: Part of the nucleus with NLB and clusters of perichromatin granules (PGs, arrows) after labeling with anti-Oct-4 antibody. Note the tight association of the labeling with granules in clusters. CH, chromatin (arrow). **D**: Double-immunogold labeling of spherical body with anti-Oct-4 antibody (small gold particles) and anti-SC 35 (large gold particles). A part of a nuclear serial section with a fragment of spherical body (SB) is presented. Note that most of labeling is adjacent to granular material of spherical body.

coincides with anti-SC 35 (Fig. 5A). Colocalization of Oct-4 with 8WG16 also occurs but on rare occasions (Fig. 5B). Anti-SC 35 labeling revealed that several small granular, irregular-shaped nuclear bodies are enriched in SC 35 (Fig. 5C), indicating that these nuclear bodies represent IGCs similar to those from oocytes of uni- and bi-laminar stages of mouse follicle development. IGCs of antral follicles also contain Oct-4 (Fig. 5D). SC 35 was also frequently found in significant concentration in PGs (Fig. 5E). Analysis of serial sections revealed that while some SC 35 labeling is associated with PGs and chromatin adjacent to NLB, the

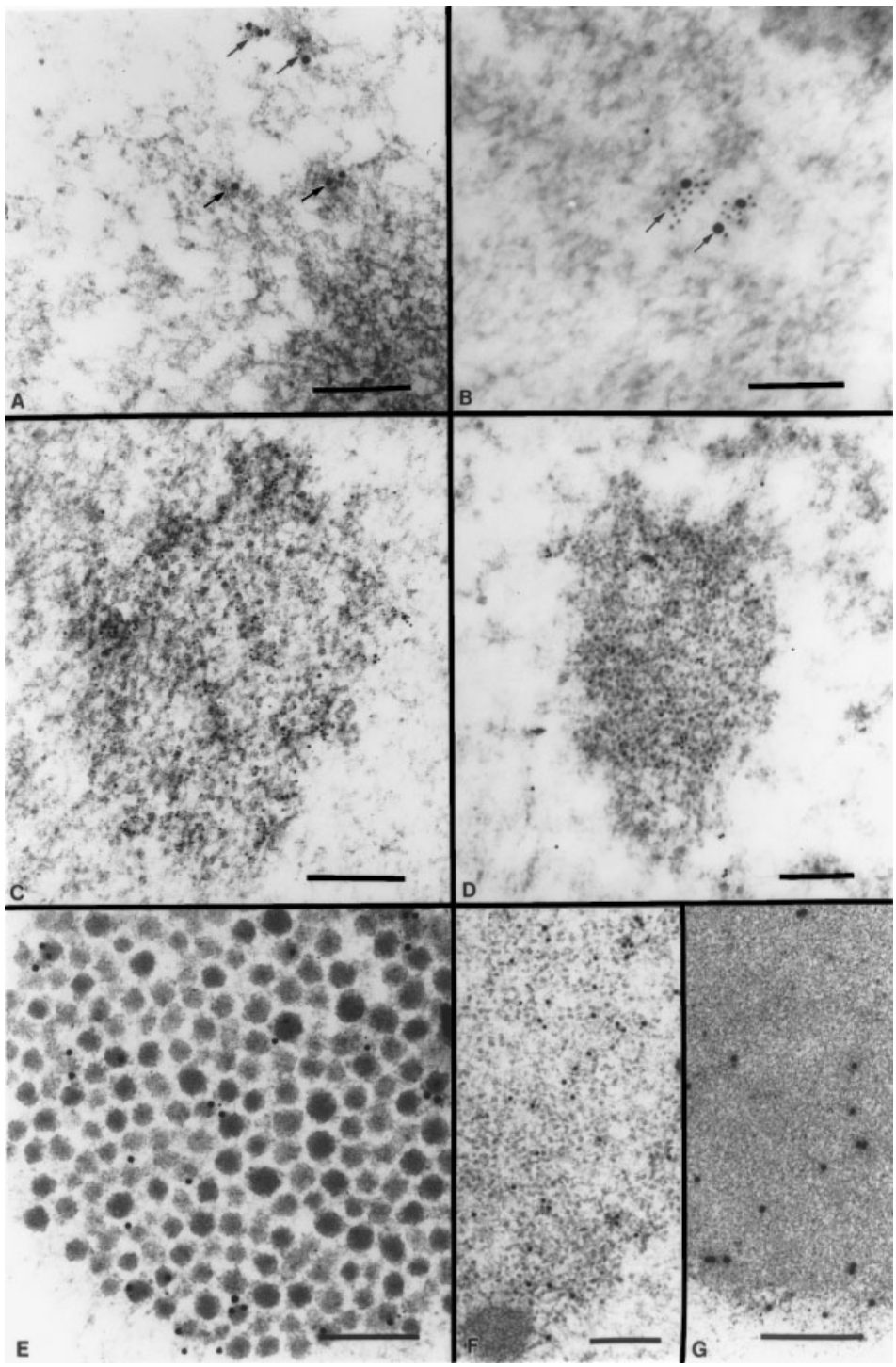

Fig. 5. Immunogold labeling of nuclear structures in inert-stage oocytes from antral follicles. **A**: Double-immunogold labeling of the karyoplasms with anti-Oct-4 (small gold particles) and anti-SC 35 (large gold particles), Note the colocalization of Oct-4 and SC 35 and their association with fibrillar material of chromatin (arrows). **B**: Double-immunogold labeling of a part of the karyoplasm with anti-Oct-4 (large gold particles) and anti-Pol II (8WG16) (small gold particles). Note the colocalization of Oct-4 and unphosphorylated form of Pol II (arrows). **C**: Labeling of irregular-shaped nuclear body with anti-SC 35. Note that this body is enriched in SC 35 indicating that it represents interchromatin granule cluster (IGC). **D**: Immunogold labeling of IGC with anti-Oct-4 antibody. IGC of mouse antral follicle accumulates Oct-4. **E**: The fragment of PGs clump after double-immunogold labeling with anti-SC 35 (large gold particles) and anti-Oct-4 (small gold particles) antibodies. **F**, **G**: Double-immunogold labeling of spherical body (F) and NLB (G) with anti-coilin (large gold particles) and anti-SC 35 (small gold particles). Note the absence of anti-SC 35 labeling in NLB (G) and occurrence both anti-coilin and anti-SC 35 in spherical body (F), which represents Cajal body (CB).

NLB itself remained unlabeled with anti-SC 35. NLBs and spherical granular bodies display a high intensity of anti-coilin labeling (Fig. 5F,G). While NLBs do not contain splicing factors (Fig. 5G), spherical bodies include both coilin and SC 35 as revealed by double labeling studies (Fig. 5F). It is difficult (even using analysis of serial sections) to rigorously prove whether there is a real colocalization between labels of two antibodies. However, we have constantly observed high frequency of association of anti-coilin with anti-SC 35 in different zones of these nuclear bodies (Fig. 5F). In the karyoplasm of this stage, sparse anti-coilin labeling distributed in a diffuse pattern.

Thus, in oocyte nuclei from antral follicles, besides NLB and clumps of PGs, we observe two types of structures containing Oct-4, irregular-shaped small fibrillo-granular (granules 20–25 nm in diameter) nuclear bodies intensively labeling with anti-SC 35 corresponding to IGCs of active stage uni-bilaminar follicles and the other, the large spherical compact nuclear bodies with the same fine morphology showing anti-SC 35 labeling but with less intensity. The important feature of these bodies is that they include the hallmark protein of CBs, the coilin (see Fig. 5F). The presence of coilin in these structures was confirmed with confocal microscopy (see below). In recent studies, the presence of coilin in nuclear bodies is recognized as the adequate criterion to define such bodies as CBs [Grande et al., 1997; Schul et al., 1998; Morgan et al., 2000). By this criterion, we designate the large spherical fibrillo-granular bodies of mouse antral follicles as CBs. (see additional notes on the composition and morphology of CBs in the Discussion).

Confocal Laser Scanning Microscopy

To confirm the immunogold labeling/electron microscopy observations, we performed studies with CLSM on squash preparations after immunofluorescent labeling. Because the uni/bilaminar follicles lie deeply in ovary tunica and are tightly bound to the connective tissue, we could not prepare satisfactory squash material from these follicles. Therefore, we conducted confocal microscopy studies on squashed oocytes from antral follicles that are easily distinguished on the surface of the mouse ovary. We first performed triple labeling studies on these oocytes to show the simultaneous staining of coilin, SC 35, and DNA. Figure 6A shows an optical section of oocyte nucleus after anti-coilin staining (FITC, green channel). Coilin is distributed diffusely throughout the oocyte and appears to accumulate in NLB and in few spherical nuclear bodies that range in diameter from 3 to 9 μ. These bodies appear to correspond to CBs described at ultrastructural level (see Figs. 3 and 5F). Figure 6B shows the same oocyte nucleus after staining with Mab SC 35 (Texas red, red channel). The nucleus has 1–2 irregular-shaped brightly labeled domains and a few spherical domains that stained weakly for SC 35. When the SC 35 labeling is compared with anti-coilin staining, it is clear that these weakly staining SC 35 domains colocalize with CBs (merged image of green and red channels, Fig. 6D). However, SC 35 is absent from the antral follicle NLBs, which are enriched in coilin. IGCs, which label with SC 35 antibody show no labeling with anti-coilin (Fig. 6B,D). The chromatin is distributed through the nucleus forming occasional condensed patches (Fig. 6C). Chromatin closely associates with coilin-containing nuclear bodies and also surrounds the NLB.

The next set of triple staining studies examined the nuclear distribution of Oct-4, SC 35, and DNA in the oocyte. In general, the nuclear distribution of Oct-4 corresponds to that of coilin (compare Fig. 6A,E). In addition to the punctuate distribution in karyoplasm, Oct-4 is concentrated in compact NLB and in several CBs (Fig. 6E). Oct-4 shows colocalization with SC 35 in CBS (Fig. 6F,H). To examine the spatial relationship between nuclear distribution of Oct-4 and Pol II, we performed a double staining experiment which showed that both proteins accumulate and colocalize in NLB (Fig. 6I,J,L). Within NLB, Pol II shows a patchy distribution.

Our observations indicate that both Oct-4 and coilin continue to be concentrated in NLB of oocytes from antral follicles to the end of their preovulatory stage. At this period, CBs disappear from the nuclei. NLB is the only distinguishable intranuclear structure containing Oct-4 and coilin; NLB preserves its compact spherical shape while a highly condensed chromatin surrounds the NLB in the form of complete ring (data not shown).

DISCUSSION

We studied here, for the first time, the intranuclear distribution of the transcription

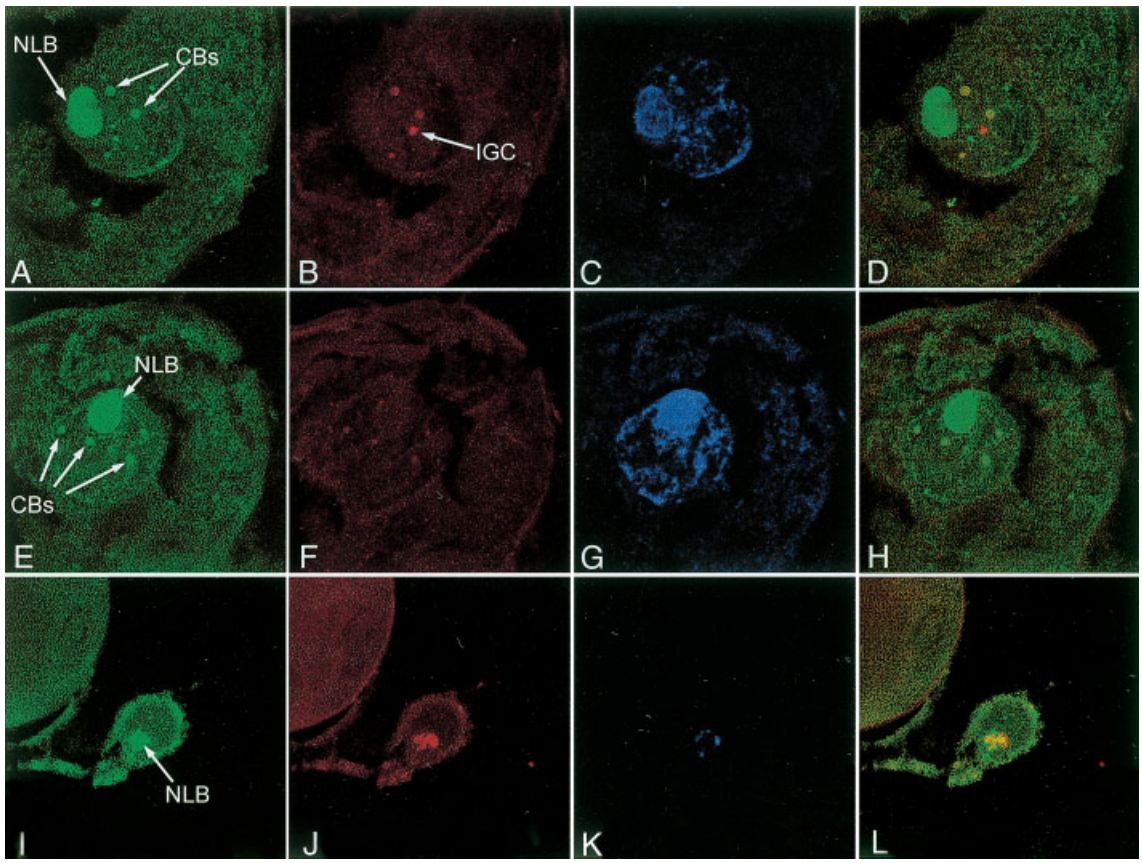

Fig. 6. Confocal laser scanning micrograph of antral follicle squash preparations stained with antibodies to coilin (**A**), SC 35 (**B**, **F**), Oct-4 (**E**, **I**), and Pol II (**J**). **Top** panel shows the same oocyte labeled with anti-coilin (green, A) and anti-SC 35 (red, B), **middle** panel shows a different oocyte labeled with anti-Oct-4 (green, E) and anti-SC 35 (red, F), and **lower** panel shows an oocyte stained with anti-Oct-4 (green, I) and anti-Pol II (red, J). **C**, **G**, **K** are images of the three oocytes stained for the nuclear DNA with TO-PRO-3. **D** is a merged image of A and B, **H** is a merged image of E and F, and **L** is a merged image of I and J. Note that these pictures are only partial images of oocytes showing mostly the nucleus and that in the oocyte shown in the left lower panel the squashing procedure separated the nucleus from the oocyte.

factor Oct-4 in relation to the transcriptional state of the mouse oocytes and in relation to other components of the transcription machinery. The key observations presented here are as follows: (i) Oct-4 in oocyte nuclei from uni- and bi- laminar mouse follicles (transcriptionally active stage) is localized in the intranuclear domains such as PFs, IGCs, and nucleolus; (ii) at active stage, Oct-4 is associated with unphosphorylated form of Pol II and splicing factor SC 35 in both PFs and IGCs; (iii) in oocyte nuclei from antral follicles (inactive stage), Oct-4 is concentrated in NLB, CBs, and PGs; NLBs also contain coilin and Pol II. CBs contain coilin, Pol II, and SC 35. PGs also contain the splicing factor, SC 35.

The presence of Oct-4 in PFs, although demonstrated by us for the first time, is not totally unexpected. A number of earlier studies have shown that PFs contain many transcription and splicing factors [Fakan et al., 1984; Spector, 1993; Kiseleva et al., 1994; Cmarko et al., 1999; Parfenov et al., 2000]. The prevailing notion is that PFs represent a distinct karyoplasmic domain involved in active pre-mRNA transcription and processing (for review see Fakan, 1994; Cmarko et al., 1999). The accumulation of Oct-4 in IGCs of active oocytes is significant. The IGCs have been analyzed biochemically and were found to contain a number of components of transcription machinery [Mintz et al., 1999]. In amphibian oocytes, Gall et al. [1999] described B-snurposomes which contain granules measuring 20–30 nm and appear to be the counterparts of IGCs described in somatic cells. It has been suggested that each of these granules termed the "Pol II transcriptosomes" contain Pol II holoenzyme in a pre-formed complex. We attribute a similar composition to the granules of IGCs of active

mouse oocytes. Thus, IGCs appear to be the sites at which the transcription/processing machinery is assembled into complex (es) prior to their transfer to PFs. Our observations on the colocalization of Oct-4 in IGCs along with Pol II and SC 35 suggest that Oct-4, a transcription factor which is not part of the holoenzyme, does associate with the transcriptosomes in the IGCs. It is interesting to identify the mechanism by which Oct-4 is recruited to the IGCs. In this context, it is noteworthy that biochemical studies have suggested that certain holoenzyme component can provide specific sites for the interaction of external transcriptional regulators [Meyer and Young, 1998; Lee and Young, 2000; Malik and Roeder, 2000]. It is possible that Oct-4 may interact with those sites and traverses to the PF with the holoenzyme.

An intriguing result in the present study is the association of Oct-4 with the nucleolus in active oocytes. The specific and consistent association of Oct-4 with the DFC of the nucleolus suggests that this result is not due to some procedural artifacts. The fact that nucleoli are neither sites of pre-mRNA synthesis nor mRNA processing makes this observation unexplainable. At present, we cannot envision a biological significance for this observation.

Concerning the distribution of Oct-4, Pol II, and SC 35 in the nuclei of inert oocytes from mouse antral follicles, our finding suggest that coilin-containing structures (NLBs and CBs) predominantly accumulate these components of transcriptional machinery. The NLBs contain Oct-4 and Pol II, but not SC 35; this confirms our earlier localization studies of Pol II and SC 35 in human oocytes from antral follicles [Parfenov et al., 1998, 2000]. Again, these results suggest a close association of Oct-4 with components of transcription and splicing machinery in the intranuclear domains as was seen in the active oocytes.

The presence of Oct-4 in NLB may be significant for other reasons. Because NLBs are the only coilin-containing structures at the end of preovulatory stages of oogenesis, they may be the major sites for the storage of transcriptional machinery. The association of Oct-4 with NLB prior to ovulation may also assure a direct transfer of the maternally inherited protein via NLB to the zygote. The possible transfer of Oct-4 from eggs to zygotes was previously postulated [Kinlosh and Wassarman, 1993]. By contrast, other coilin-containing structures such as CBs may not play such a role because they are transient structures. We have shown that CBs disappear in the oocytes of preovulatory follicles confirming certain earlier studies [Chouinard, 1975]. Such behavior of CBs during the late prophase I of meiosis (preovulatory stage) on the background of the transcription reduction is consistent with the data on disappearance of CBs from somatic prophase in mitosis [Andrade et al., 1993; Ferreira et al., 1994] and disruption of CBs by transcription inhibition [Carmo-Fonseca et al., 1992].

Finally, we need to explain the presence of SC 35 in the CBs of antral follicle oocytes. Although this splicing factor has not been demonstrated in CBs of somatic cells [Matera, 1999], certain line of evidence from an analysis of oocytes indicates the presence of SC 35 in CBs. A weak staining with anti-SC 35 was observed in amphibian oocyte CB in spreads of nuclei [Gall et al., 1999] or in spreads after injection of anti-SC 35 into nuclei [Bellini and Gall, 1999]. CBs containing notable amount of SC 35 were observed in oocytes of insects [Batalova et al., 2000; Bogolyubov and Parfenov, 2001]. The possibility cannot be excluded that in somatic cells and oocytes, CBs differ in composition and probably in organization. A case in point is the notable diversity in morphology of CBs among different species of insects; some have CBs in the form of large sphere-shaped bodies [Tsvetkov et al., 1997] consisting of fibrillar material while others have CBs composed of distinct granular material [Bogolyubov et al., 2000; Bogolyubov and Parfenov, 2001].

ACKNOWLEDGMENTS

We thank Dr. Joan Steitz for the Y12 antibody, Dr. X-D. Fu and Dr. T. Maniatis for anti-SC 35 antibody, Dr. E. K. L. Chan for anti-coilin antibidy. We are grateful to Dr. Alexey Tomilin and Vladimir Vorobyev for stimulating discussions. This research was supported by Cancer Center Support (CORE) grant CA-21765, American Lebanese Syrian Associated Charities (K.G.M), and Russian Fund for Basic Research, Grant # 00-04-49121(V.P.).

REFERENCES

Andrade LEC, Tan EM, Chan EKL. 1993. Immunocytochemical analysis of the coiled body in the cell cycle and during cell proliferation. Proc Natl Acad Sci USA 90: 1947–1951.

Antoine N, Lepoint A, Baeckeland E, Goessens G. 1988. Ultrastructural cytochemistry of the nucleolus in rat oocytes at the end of the folliculogenesis. Histochemistry 89:221–226.

Batalova FM, Stepanova IS, Bogolyubov DS. 2000. Cajal bodies in oocyte nuclei of the scorpion fly *Panorpa communis*. Tsitologiia 41:1037–1047.

Bauer DW, Gall JG. 1997. Coiled bodies without coilin. Mol Biol Cell 8:73–82.

Bellini M, Gall JG. 1999. Coilin shuttles between the nucleus and cytoplasm in *Xenopus* oocytes. Mol Biol Cell 10:3425–3434.

Bogolyubov D, Parfenov VN. 2001. Immunogold localization of RNA polymerase II and pre-mRNA splicing factors in *Tenebrio molitor* oocytes nuclei with special emphasis on karyosphere development. Tissue and Cell 33:1–13.

Bogolyubov D, Alexandrova O, Tsvetkov A, Parfenov VN. 2000. An immunoelectron study of karyosphere and nuclear bodies in oocytes of mealworm beetle, *Tenebrio molitor* (Coleoptera: Polyphaga) Chromosoma 109:415–425.

Carmo-Fonseca M, Pepperkok R, Carvalho MT, Lamond A. 1992. Transcription-dependent colocalization of the U1, U2, U4/U6, and U5 snRNPs in coiled bodies. J Cell Biol 117:1–14.

Chouinard LA. 1975. A light and electron-microscope study of the oocyte nucleus during development of the antral follicle in the prepubermal mouse. J Cell Sci 17:589–615.

Cmarko D, Verschure PJ, Martin TE, Dahmus M, Krause S, Fu X-D, van Driel R, Fakan S. 1999. Ultrastructural analysis of transcription and splicing in the cell nucleus after bromo-UTP microinjection. Mol Biol Cell 10:211–223.

Daskal Y. 1981. Perichromatin granules. In: The cell nucleus. Vol. 8. New York: Academic Press. 117–140.

Debey P, Szöllösi M.S, Szöllösi D, Vautier D, Girousse A, Besombes D. 1993. Competent mouse oocytes isolated from antral follicles exhibit different chromatin organization and follow different maturation dynamics. Mol Reprod Dev 36:59–74.

Dundr M, Misteli T. 2001. Functional architecture in the cell nucleus. Biochem J 356:297–310.

Fakan S. 1994. Perichromatin fibrils are in situ forms of nascent transcripts. Trends Cell Biol 4:86–90.

Fakan S, Puvion E. 1980. The ultrastructural visualization of nucleolar and extranucleolar RNA synthesis and distribution. Int Rev Cytol 65:255–299.

Fakan S, Leser G, Martin TE. 1984. Ultrastructural distribution of nuclear ribonucleoproteins as visualized by immunocytochemistry on thin sections. J Cell Biol 98: 358–362.

Ferreira JA, Carmo-Fonseca M, Lamond AL. 1994. Differential interaction of splicing snRNPs with coild bodies and interchromatin granules during mitosis and assembly of daughter cell nuclei. J Cell Biol 126:11–23.

Fong N, Bentley DL. 2001. Capping, splicing, and 3′ processing are independently stimulated by RNA polymerase II: Different functions for different segments of the CTD. Genes Dev 15:1783–1179.

Gall JG. 2000. Cajal bodies: The first 100 years. Annu Rev Cell Dev Biol 16:273–300.

Gall JG, Bellini M, Wu Z, Murphy C. 1999. Assembly of the nuclear transcription and processing machinery: Cajal bodies (Coiled bodies) and transcriptosomes. Mol Biol Cell 10:4385–4402.

Grande MA, van der Kraan J, de Jong L, Driel R. 1997. Nuclear distribution of transcription factors in relation to sites of transcription and RNA polymerase II. J Cell Sci 110:1781–1791.

Greenblatt J. 1997. RNA polymerase II holoenzyme and transcriptional regulation. Curr Opin Cell Biol 9: 310–319.

Kaplan G, Abreu SL, Bachvarova R. 1982. rRNA accumulation and protein synthesis in growing mouse oocytes. J Exp Zool 220:361–370.

Kinlosh RA, Wassarman PM. 1993. Specific gene expression during oogenesis in mice. In: Gwatkin RBL, editor. Genes in mammalian reproduction 27–43. New York, NY: Wiley-Liss, Inc.

Kiseleva E, Wurtz T, Visa N, Duneholt B. 1994. Assembly and dissassembly of spliceosomes along a specific pre-mRNP fiber. EMBO J 13:6052–6061.

Koleske AJ, Young RA. 1995. The RNA polymerase II holoenzyme and its implications for gene regulation. Trends Biochem Sci 20:113–116.

Kopecny V, Biggiogera M, Laurincik J, Pivko J, Grafenau P, Martin TE, Fu XD, Fakan S. 1996. Fine structural cytochemical and immunocytochemical analysis of nucleic acids and ribonucleoprotein distribution in nuclei of pig oocytes and early preimplantation embryos. Chromosoma 104:561–574.

Lee TJ, Young RA. 2000. Transcription of eukaryotic protein-coding genes. Annu Rev Genet 34:77–137.

Malik S, Roeder RG. 2000. Trancriptional regulation through mediator-like coactivators in yeast and metazoan cells. Trends Biochem Sci 25:277–283.

Matera AG. 1999. Nuclear bodies: Multifaceted subdomains of the interchromatin space. Trends Cell Biol 9: 302–309.

Mc Craken S, Rosonina E, Fong N, Sikes M, Beyer A, O' Hare K, Shuman S, Bently D. 1998. Role of RNA polymerase II carboxy-terminal domain in coordinating transcription with RNA processing. Cold Spring Harbor Symp Quant Biol 7:135–138.

Meyer VE, Young RA. 1998. RNA polymerase II holoenzymes and subcomplexes. J Biol Chem 273:27757–27760.

Mintz PS, Patterson SD, Neuwald AF, Spahr CS, Spector DL. 1999. Purification and biochemical characterization of interchromatin granule clusters. EMBO J 18:4308–4320.

Misteli T. 2000. Cell biology of transcription and pre-mRNA splicing: Nuclear architecture meets nuclear function. J Cell Sci 113:1841–1849.

Moore GPM, Lintern-Moore S, Peters H, Faber M. 1974. RNA synthesis in mouse oocyte. J Cell Biol 60:416–422.

Morgan GT, Doyle O, Murphy C, Gall JG. 2000. RNA polymerase II in Cajal bodies of amphibian oocytes. J Struct Biol 129:258–268.

Murti KG, Brown PS, Kumagai M, Campana D. 1996. Molecular interactions between human B-cell progenitors and the bone marrow microenvironment. Exp Cell Res 226:47–58.

Palmieri SL, Peter W, Hess H, Schöler HR. 1994. Oct-4 transcription factor is differentially expressed in the mouse embryo during establishment of the first two extraembryonic cell lineages involved in implantation. Dev Biol 166:259–267.

Parfenov VN, Davis DS, Pochukalina GN, Sample CE, Murti KG. 1996. Nuclear bodies of stage 6 oocytes of

Rana temporaria contain nucleolar and coiled body proteins. Exp Cell Res 228:229–236.

Parfenov VN, Davis DS, Pochukalina GN, Kostyuchek DF, Murti KG. 1998. Dynamics of distribution of splicing components relative to the transcriptional state of human oocyte from antral follicles. J Cell Biochem 69:72–80.

Parfenov VN, Davis DS, Pochukalina GN, Kostyuchek DF, Murti KG. 2000. Nuclear distribution of RNA polymerase II in human oocytes from antral follicles: Dynamics relative to the transcriptional state and association with splicing factors. J Cell Biochem 77:654–665.

Pesce M, Schöler HR. 2000. Oct-4: Control of totipotency and germline determination. Mol Reprod Dev 55:452–457.

Pesce M, Wang X, Wolgemuth DJ, Schöler H. 1998. Differential expression of the Oct-4 transcription factor during mouse germ cell differentiation. Mech Dev 71:89–98.

Peters H. 1969. The development of the mouse ovary from birth to maturity. Acta Endocr 62:98–116.

Quinn P, Barros C, Whittingham DG. 1982. Preservation of hamster oocytes to assay the fertilizing capacity of human spermatozoa. J Reprod Fertil 66:161–168.

Schul W, Driel R, de Jong L. 1998. Coiled bodies and U2 snRNA genes adjacent to coiled bodies are enriched in factors required for snRNA transcription. Mol Biol Cell 9:1025–1036.

Schöler HR. 1991. Octamania: The POU factors in murine development. Trend Genet 7:323–329.

Spector DL. 1993. Macromolecular domains within the cell nucleus. Annu Rev Cell Biol 9:265–315.

Szöllösi M, Debey P, Szöllösi D, Rime H, Vautier D. 1991. Chromatin behavior under influence of puromycin and G-DMAP at different stages of mouse oocytes maturation. Chromosoma 100:339–354.

Tsvetkov A, Alexandrova O, Bogolyubov D, Gruzova M. 1997. Nuclear bodies cricket and mealworm oocytes contain splicing factors of pre-mRNA. Eur J Entomol 94:394–407.

Zatsepina OV, Bouniol-Baly Ch, Amirand C, Debey P. 2000. Functional and molecular reorganization of the nucleolar apparatus in maturing mouse oocytes. Dev Biol 223:354–370.

Zybina EV. 1971. The synthesis of RNA and protein in the oocyte and follicle of mice. Tsitologiia 13:768–775.